

# Spin excitations under fields in an anisotropic bond-alternating quantum $S=1$ chain: contrast with Haldane spin chains

M. Hagiwara<sup>1,\*</sup>, L. P. Regnault<sup>2</sup>, A. Zheludev<sup>3</sup>, A. Stunault<sup>4</sup>,  
N. Metoki<sup>5</sup>, T. Suzuki<sup>6</sup>, S. Suga<sup>6</sup>, K. Kakurai<sup>5</sup>, Y. Koike<sup>5</sup>, P. Vorderwisch<sup>7</sup>, and J. H. Chung<sup>8\*</sup>

<sup>1</sup>RIKEN(The Institute of Physical and Chemical Research), Wako, Saitama 351-0198, Japan

<sup>2</sup>CEA-Grenoble, DRFMC-SPSMS-MDN, 17 rue des Martyrs, 38054 Grenoble Cedex 9, France

<sup>3</sup>Condensed Matter Sciences Division, Oak Ridge National Laboratory, Oak Ridge, Tennessee 37831-6393, USA

<sup>4</sup>Institut Laue Langevin, 6 rue J. Horowitz, 38042 Grenoble Cedex 9, France

<sup>5</sup>JAERI, Advanced Science Research Center, Tokai, Ibaraki 319-1195, Japan

<sup>6</sup>Department of Applied Physics, Osaka University, Suita, Osaka 565-9871, Japan

<sup>7</sup>BENSC, Hahn-Meitner Institut, D-14109 Berlin, Germany

<sup>8</sup>NIST Center for Neutron Research, National Institute of Standards and Technology, Gaithersburg, Maryland 20899, USA

(Dated: December 19, 2018)

Inelastic neutron scattering experiments on the  $S=1$  quasi-one-dimensional bond-alternating antiferromagnet  $\text{Ni}(\text{C}_9\text{D}_{24}\text{N}_4)(\text{NO}_2)\text{ClO}_4$  have been performed under magnetic fields below and above a critical field  $H_c$  at which the energy gap closes. Normal field dependence of Zeeman splitting of the excited triplet modes below  $H_c$  has been observed, but the highest mode is unusually small and smears out with increasing field. This can be explained by an interaction with a low-lying two magnon continuum at  $q_{\parallel} = \pi$  that is present in dimerized chains but absent in uniform ones. Above  $H_c$ , we find only one excited mode, in stark contrast with three massive excitations previously observed in the structurally similar Haldane-gap material NDMAP [A. Zheludev et al., Phys. Rev. B **68**, 134438 (2003)].

PACS numbers: 75.40.Gb, 75.10.Jm, 75.50.Ee

Recent experimental advances allowed studies of a new exciting phenomenon, namely field-induced Bose condensation of magnons in gapped quantum magnets [1]. Particularly interesting is the case of antiferromagnetic  $S = 1$  spin chains. For uniform chains the ground state is an exotic *quantum spin liquid* with only short-range spin correlations and a gap in the excitation spectrum [2]. Antiferromagnetic  $S = 1$  chains that are not uniform, but instead feature alternating strong and weak bonds, are also gapped spin liquids except at a quantum critical point [3]. However, for sufficiently strong alternation their so-called dimerized ground state is *qualitatively distinct* from the Haldane state [4, 5, 6, 7, 8]. The differences are significant yet subtle, and involve the breaking of the so-called “hidden” symmetry. This symmetry is related to a non-local topological “string” order parameter [9, 10] that is *in principle* not observable experimentally. For example, thermodynamic properties are expected to be almost identical for Haldane and dimerized cases. Moreover, field-induced Bose condensation of magnons occurs in both types of spin chains and is expected to lead them into *the same* (in terms of preserved symmetries of the wavefunction) magnetized high-field state [11]. Thus, at a first glance, for the Haldane and the dimerized spin chains one can expect the spin dynamics to be similar in a wide range of external fields. *But is it indeed true?*

The recently discovered [12] nickel chain material  $\text{Ni}(\text{C}_9\text{H}_{24}\text{N}_4)(\text{NO}_2)\text{ClO}_4$ , abbreviated to NTENP, offers an ideal experimental approach to the above problem. NTENP features bond-alternating  $S=1$  antiferromagnetic chains in the gapped dimerized phase,

as shown by magnetization and ESR measurements [8], and neutron scattering experiments [13, 14]. It is structurally similar to the Haldane materials NENP ( $\text{Ni}(\text{C}_2\text{H}_8\text{N}_2)_2(\text{NO}_2)\text{ClO}_4$ ) and NDMAP ( $\text{Ni}(\text{C}_5\text{H}_{14}\text{N}_2)_2\text{N}_3(\text{PF}_6)$ ) whose field behavior was previously extensively investigated [15, 16, 17]. NTENP also has comparable anisotropy and energy scales, which allows a direct comparison between these systems. In the present study we performed neutron scattering experiments on 98% deuterated NTENP in a wide range of applied fields. We clearly observed Zeeman splitting of the excited triplet states below  $H_c$ , a field-induced softening of the spin gap, and the resulting emergence of antiferromagnetic long range order (LRO) above  $H_c$  [18], similar to what is seen in NDMAP. However, certain features of the spin excitation spectrum in NTENP are substantially different. Notable differences in the spin correlation function are present already at  $H = 0$ , with even more striking discrepancies becoming prominent at  $H > H_c$ .

First we summarize the crystal and magnetic properties of NTENP. This compound crystallizes in the triclinic system (space group  $P\bar{1}$ ) [12] with lattice constants  $a=10.747(1)\text{\AA}$ ,  $b=9.413(2)\text{\AA}$ ,  $c=8.789(2)\text{\AA}$ ,  $\alpha=95.52(2)^\circ$ ,  $\beta=108.98(3)^\circ$  and  $\gamma=106.83(3)^\circ$  [12]. The  $\text{Ni}^{2+}$  ions are bridged by nitrito groups along the  $a$  axis having two different bond distances of  $2.142(3)$  and  $2.432(6)\text{\AA}$ . These chains are weakly coupled via intervening perchlorate counter anions. The inversion centers are situated not on the  $\text{Ni}^{2+}$  ions but on the nitrito groups, so that no staggered components of the magnetic moments are expected to be retained, thus resulting in occurrence of the

long range order above  $H_c$  at low temperatures [18] like in NDMAP [20, 21]. The model spin hamiltonian is written as:

$$\mathcal{H} = \sum_i [J\mathbf{S}_{2i-1} \cdot \mathbf{S}_{2i} + \delta J\mathbf{S}_{2i} \cdot \mathbf{S}_{2i+1} - \mu_B \mathbf{S}_i \tilde{g} \mathbf{H} + D(S_i^z)^2], \quad (1)$$

where  $J$  is the large exchange constant,  $\mathbf{S}_{2i-1}$ ,  $\mathbf{S}_{2i}$  and  $\mathbf{S}_{2i+1}$  the  $S=1$  spin operators,  $\delta$  the bond-alternating ratio,  $\tilde{g}$  the  $g$  tensor of  $\text{Ni}^{2+}$ ,  $\mu_B$  the Bohr magneton and  $\mathbf{H}$  an external magnetic field, and  $D$  is a single ion anisotropy constant. From the analysis of the magnetic susceptibility data, the following parameter values were evaluated from a comparison with numerical calculations [8]: the large exchange constant  $J/k_B = 54.2$  K, the bond alternating ratio  $\delta=0.45$ , the single ion anisotropy constant  $D/J = 0.25$  ( $D/k_B=13.6$  K), and  $g_{\parallel}=2.14$  for the chain direction. A similar bond-alternating ratio was also evaluated in Inelastic Neutron Scattering (INS) measurements [13, 14]. Such a bond alternating ratio corresponds to the ground state in the dimer phase. This conclusion was directly confirmed by magnetization, ESR [8] and INS [13] experiments on NTENP.

Three large single crystal samples NTENP with a typical size of  $16 \times 12 \times 4$  mm<sup>3</sup> were prepared for the current study by the method described in Ref. 12. The mosaic spread of the sample was typically about  $1.2^\circ$ . The INS measurements were performed on several three-axis spectrometers installed at different cold and thermal neutron sources (IN8, IN12, IN14 and IN22 at ILL-Grenoble, V2 at HMI-Berlin, SPINS at NIST center for neutron research and LTAS at JAERI). Specific details will be reported elsewhere. The scattering plane was the  $(a^*, c^*)$  plane and the external magnetic field was applied to the  $b$  axis. Hence, the field direction was not perpendicular to the chain direction ( $a$  axis) ( $\gamma = 106.83(3)^\circ$ ). In this configuration, the  $a^*$  was tilted from the  $a$  axis by  $\approx 30^\circ$  and the field dependence of the  $(1,0,0)$  magnetic Bragg peak measured at 100 mK clearly indicated a field-induced ordering transition at  $H_c \approx 11.3$  T (Fig.1(a)).

As a first step in our investigation we characterized the system at zero field. In agreement with previous studies [13], we observed three distinct branches of gap excitations that appear as resolution-limited peaks in constant- $q$  scans at the 1D AF zone-center. These data are shown in symbols in the upper panel of Fig. 2. Lines represent contributions of each mode, as calculated in the Single Mode Approximation (SMA), assuming a parabolic dispersion along the chain axis and fully taking into account resolution effects, as was previously done in Ref. [13]. Each of the three observed peaks corresponds to a particular member of the  $S = 1$  excitation triplet that even at  $H = 0$  is split by single-ion anisotropy. The three gap energies were estimated to be  $1.06 \pm 0.01$ ,  $1.15 \pm 0.01$  and  $1.96 \pm 0.01$  meV, respectively. The dispersion of the lower modes was measured all the way to the zone-boundary,

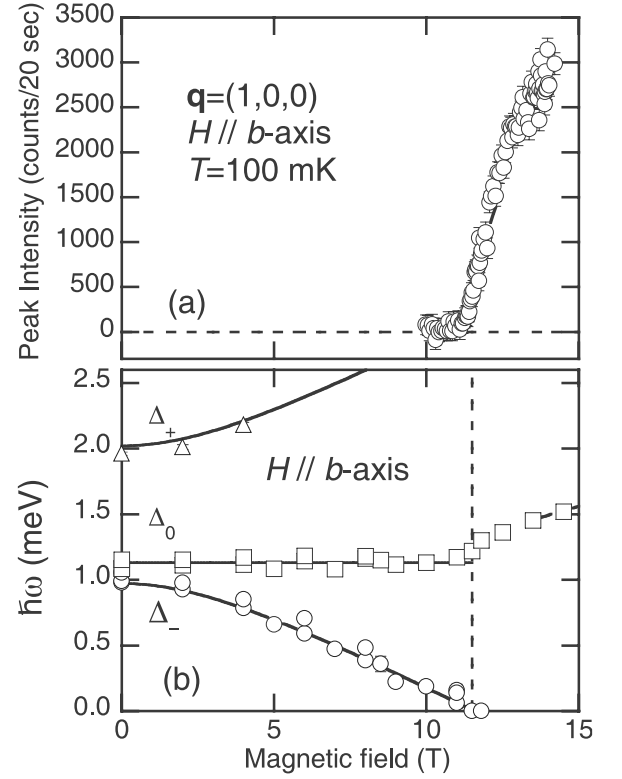


FIG. 1: (a) Field dependence of the magnetic Bragg peak intensity at  $\mathbf{q}=(1,0,0)$ . The solid line is a fit of the experimental data to the expression  $a(H-H_c)^{2\beta_c}$  with  $H_c=11.35$  T and  $\beta_c=0.316$  between 11.3 T and 12 T. The  $\beta_c$  value is close to the expected 3D-XY value. The dashed line is a guide for the eyes. (b) Field dependence of the gap energies measured in NTENP. Solid lines are calculated triplet branches in a magnetic field and a vertical thin broken line indicates the critical field  $H_c$ . The line above  $H_c$  is a guide for the eyes.

as shown by a solid line in the main panel of Fig. 3. It is well described by the form  $(\hbar\omega)^2 = \Delta^2 + \omega_{\max}^2 \sin^2 \pi h$ , where the wave vector transfer  $\mathbf{q} = (h, k, l)$ ,  $\Delta = 1.1$  meV and  $\omega_{\max} = 7.2$  meV. The higher-energy mode (a broken line) follows a similar dispersion curve with  $\Delta = 2.2$  meV and  $\omega_{\max} = 7.2$  meV. Apart from a somewhat larger gap energy and bandwidth, the observed behavior appears to be very similar to that previously seen in NDMAP[22].

The first key new finding of the present study is that at  $H = 0$  the relative intensity of the higher-energy member of the triplet is anomalously weak. This fact is consistent with the data shown in Ref. 13, but was previously overlooked. Polarization effects aside, the intensity of all three components of the triplet in NDMAP scale as  $1/\omega$  to a very good approximation. Through application of the 1-st moment sum rule for  $S(\mathbf{q}, \omega)$  [23], it can be shown that such behavior directly follows from the SMA, provided that  $(D/J)^2 \ll 1$ . Experimentally, for NTENP (where  $D/J$  is actually smaller than in NDMAP) this scaling is violated, and the relative intensity of the upper mode is lower than expected by about a factor of 3. We

came to this conclusion after performing measurements in several Brillouin zones maintaining  $q_{\parallel} = \pi$ , to eliminate the effect of polarization-dependent coefficients in the unpolarized neutron scattering cross section.

The suppression of the upper mode in NTENP becomes even more apparent in applied magnetic fields. The two lower modes in NTENP behave almost exactly as in NDMAP for  $H$  applied perpendicular to the spin chains. However, unlike in NDMAP, the upper mode in NTENP vanishes in relatively modest applied fields of  $H \gtrsim 4$  T. This is borne out in the constant- $q$  scans shown in the two lower panels of Fig. 2. Thus, even well below  $H_c$  the excitation spectra of NTENP and NDMAP are *qualitatively* different. It is interesting that while the intensities of excitations in NTENP behave anomalously, the field dependencies of the corresponding gap energies at  $H < H_c$  are very similar to those in NDMAP. These field dependencies measured in NTENP are plotted in Fig. 1(b). As in the case of NDMAP, below  $H_c$  these data are well described by a simple-minded perturbation theory calculation [24]:  $\Delta_{\pm}(H) = \frac{\Delta_z + \Delta_y}{2} \pm [(\frac{\Delta_z - \Delta_y}{2})^2 + (g\mu_B H)^2]^{1/2}$  and  $\Delta_0(H) = \Delta_x$ , where  $\Delta_x$ ,  $\Delta_y$  and  $\Delta_z$  are the gaps at  $H = 0$  for excitations polarized along  $x$ ,  $y$  and  $z$ , respectively. The best fit is obtained with  $\Delta_z = 2.0 \pm 0.1$  meV,  $\Delta_x = 0.97 \pm 0.02$  meV,  $\Delta_y = 1.13 \pm 0.02$  and  $g = 2.09$ .

The second crucial finding of this work is that at  $H > H_c$  there is *only one* low-energy mode at  $q_c = \pi$  in NTENP. This can be seen from Fig. 4 that shows constant- $q$  scans collected below (8.5 T), around (11.5 T) and above (14.5 T) the critical field ( $H_c \sim 11.3$  T). These data are in stark contrast with similar scans measured in NDMAP (Fig. 1 of Ref.16), where *three* distinct modes are visible at  $H > H_c$ . As discussed above, the upper mode in NTENP vanishes well below  $H_c$ . In addition, in NTENP the lowest-energy mode that goes soft at  $H_c$  *does not reappear at higher fields*, as it does in NDMAP. The data for NTENP at 14.5 T show only a statistically insignificant hint of a peak at 0.4 meV. Scans in several Brillouin zones confirmed that the low-energy mode is absent at  $H > H_c$  in NTENP in all polarization channels.

Comparing the behaviors of NTENP and NDMAP, we conclude that the spin dynamics of anisotropic Haldane and dimerized  $S=1$  chains are qualitatively different both below and above the critical field. This fact is confirmed by a recent Lanczos first-principles study of the dynamic structure factors in NTENP and NDMAP, based on actual measured exchange and anisotropy parameters [25]. The calculated dispersion relations for NTENP (solid symbols in Fig. 3) match our experimental data remarkably well. The solid squares and circles correspond to peaks in the dynamic structure factors for excitations polarized parallel to the easy plane ( $S^{xx}$  and  $S^{yy}$ ) or perpendicular to it ( $S^{zz}$ ), respectively. The calculations also predict that at  $H = 0$  the intensity of the out-of-plane  $S^{zz}$  mode is only 20% of that for  $S^{xx}$ , in agreement with

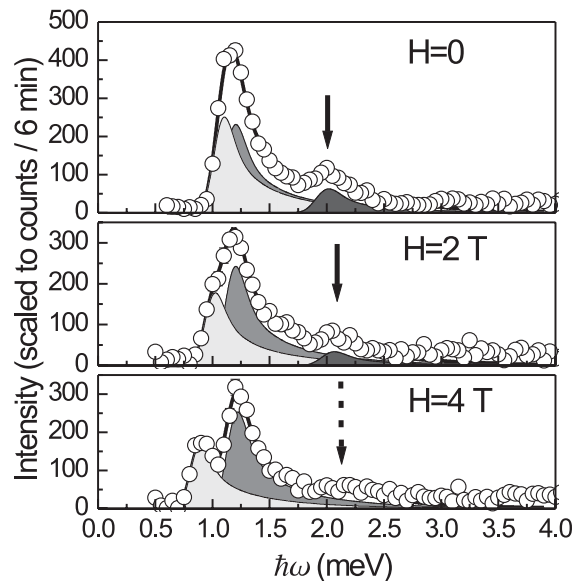


FIG. 2: Inelastic energy scans near  $\mathbf{q}=(1,0,1.5)$  at 100 mK and  $H=0, 2$  and  $4$  T.

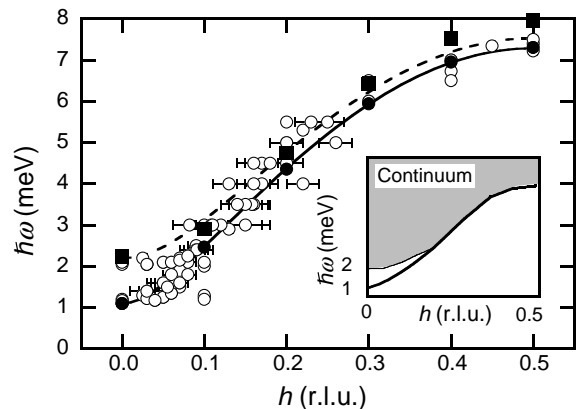


FIG. 3: Measured dispersion relation of magnetic excitations in NTENP (open circles). Solid symbols show the positions of peaks in the in-plane (squares) and out-of-plane (circles) dynamic structure obtained by Lanczos calculations. Solid and broken lines are the results of fitting to the form  $(\hbar\omega)^2 = \Delta^2 + \omega_{\max}^2 \sin^2 \pi h$ . Inset: excitation continuum (shaded area), as calculated for NTENP. The lower bound (thin solid line) coincides with the observed position of the observed  $z$ -axis mode (the highest excitation mode). The in-plane modes are shown by a heavy solid line.

the neutron results. Finally, the numerical calculations reproduce the key features at  $H > H_c$ : three modes for NDMAP and only one for NTENP.

An understanding of the underlying physical mechanism emerged from a numerical size-dependence analysis [26] that can distinguish between long-lived single-particle excitations and peaks in multi-particle continua. The key lies in the *violation of translational symmetry* in a dimerized chain. This symmetry breaking makes the

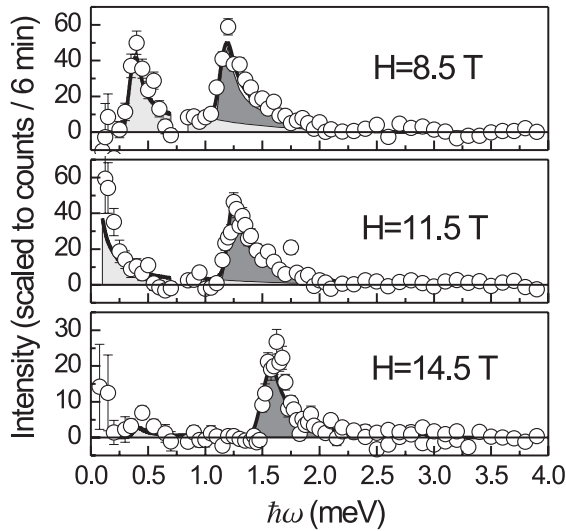


FIG. 4: Inelastic energy scans at  $\mathbf{q}=(1.1,0,1.5)$  and 100 mK for  $H=8.5$  ( $< H_c$ ),  $11.5$  ( $\sim H_c$ ) and  $14.5$  T ( $> H_c$ ).

wave vectors  $q_{\parallel} = \pi$  and  $q_{\parallel} = 0$  equivalent. As a result, in NTENP around  $q=\pi$  there is a low-lying continuum that consists of paired  $q_{\parallel} = 0$  and  $q_{\parallel} = \pi$  magnons. In the presence of sufficiently strong anisotropy the upper mode at  $q_{\parallel} = \pi$  is pushed up in energy and can enter this continuum. Once this happens, its decay into a pair of lower-energy excitations becomes allowed by energy-momentum conservation laws. The upper mode is then no longer a sharp  $\delta$ -function of energy, but appears as an asymmetric finite-width peak on the lower continuum bound (Fig. 3, inset). The situation becomes progressively worse when an external magnetic field drives the upper mode to still higher energies, deeper into the continuum. The two lower modes remain safely below the lower continuum bound at all times and are thus not affected. This scenario is reminiscent to that for the classical antiferromagnet TMMC [27]. In the latter, one magnon optic mode interacts with the two magnon mode to show the avoided crossing. However, the analogy is only superficial, since, unlike in TMMC, the single-particle excitations in NTENP are a triplet to begin with.

Nothing of the sort can occur in the uniform Haldane spin chains of NDMA, where the magnon gap at  $q_{\parallel} = 0$  is much larger than that at  $q_{\parallel} = \pi$  [26]. The lowest-energy continuum states at  $q_{\parallel} = \pi$  are then three-magnon excitations, and the corresponding continuum gap is much larger [26]. Even in the presence of anisotropy all three branches are below the continuum bounds, and persist as a triplet of long-lived excitations [28].

A low-lying continuum is also responsible for the “disappearance” of two of the three modes in NTENP at  $H > H_c$ . Numerical calculations show that, unlike below the critical field, at  $H > H_c$  the lower bound of the continuum in  $S^{zz}$  is actually beneath the lowest single-

particle state. Since at any  $H > 0$  both the highest- and lowest-energy modes have mixed polarization in the  $(y, z)$  plane, in the high-field phase they *both* become subject to decay into multi-particle states. At  $H > H_c$  only the middle mode survives in NTENP, being polarized along  $x$ . For this excitation all decay channels remain closed.

In conclusion, our experimental results clearly demonstrate fundamental quantum-mechanical differences between the two exotic spin-liquid phases of uniform and bond-alternating integral spin chains.

*Acknowledgments.*— This work was in part supported by the Molecular Ensemble research program from RIKEN and the Grant-in-Aid for Scientific Research on Priority Areas(B): Field-Induced New Quantum Phenomena in Magnetic Systems (No.13130203) from the Japanese Ministry of Education, Culture, Sports, Science and Technology. Work at ORNL was carried out under DOE Contract No. DE-AC05-00OR22725. Experiments at NIST were supported by the NSF through DMR-0086210 and DMR-9986442. The high-field magnet at NIST was funded by NSF through DMR-9704257.

- 
- \* Present address: KYOKUGEN, Osaka University, 1-3 Machikaneyama, Toyonaka 560-8531, Japan
- [1] T. Nikuni, M. Oshikawa, A. Oosawa and H. Tanaka, Phys. Rev. Lett. **84**, 5868 (2000).
  - [2] F. D. M. Haldane, Phys. Lett. A **93**, 464 (1983); Phys. Rev. Lett. **50**, 1153 (1983).
  - [3] M. Hagiwara *et al.*, Phys. Rev. Lett. **80**, 1312 (1998).
  - [4] I. Affleck and F. D. M. Haldane, Phys. Rev. B **36**, 5291 (1987).
  - [5] R. R. P. Singh and M. P. Gelfand, Phys. Rev. Lett. **61**, 2133 (1988).
  - [6] Y. Kato and A. Tanaka, J. Phys. Soc. Jpn. **63**, 1277 (1994).
  - [7] S. Yamamoto, Phys. Rev. B **52**, 10170 (1995).
  - [8] Y. Narumi, M. Hagiwara, M. Kohno and K. Kindo, Phys. Rev. Lett. **86**, 324 (2001).
  - [9] M. den Nijs and K. Rommelse, Phys. Rev. B **40**, 4709 (1989).
  - [10] T. Kennedy and H. Tasaki, Phys. Rev. B **45**, 304 (1992).
  - [11] T. Tonegawa *et al.*, J. Phys. Soc. Jpn. **65**, 3317 (1996).
  - [12] A. Escuer *et al.*, J. Chem. Soc. Dalton Trans. 531 (1997).
  - [13] A. Zheludev *et al.*, Phys. Rev. B **69**, 144417 (2004).
  - [14] L. P. Regnault *et al.*, Physica B (2004).
  - [15] L. P. Regnault, I. Zaliznyak, J. P. Renard and C. Vettier, Phys. Rev. B **50**, 9174 (1994).
  - [16] A. Zheludev *et al.*, Phys. Rev. B **68**, 134438 (2003).
  - [17] A. Zheludev *et al.*, Phys. Rev. B **69**, 054414 (2004).
  - [18] N. Tateiwa *et al.*, Physica B **329-333**, 1209 (2003).
  - [19] M. Hagiwara, Z. Honda, K. Katsumata, A. K. Kolezhuk and H. J. Mikeska, Phys. Rev. Lett. **91**, 177601 (2003).
  - [20] Z. Honda, H. Asakawa and K. Katsumata, Phys. Rev. Lett. **81**, 2566 (1998).
  - [21] Z. Honda, K. Katsumata, Y. Nishiyama and I. Harada, Phys. Rev. B **63**, 064420 (2001).
  - [22] A. Zheludev *et al.*, Phys. Rev. Lett. **88**, 077206 (2002).

- [23] P. C. Hohenberg and W. F. Brinkman, Phys. Rev. B **10**, 128 (1974).
- [24] O. Golinelli *et al.*, J. Phys.: Condens. Matter. **5**, 7847 (1993).
- [25] T. Suzuki and S. I. Suga, Phys. Rev. B **68**, 134429 (2003)
- and preprint.
- [26] M. Takahashi, Phys. Rev. B **50**, 3045 (1994).
- [27] I. U. Heilmann *et al.*, Phys. Rev. B **24**, 3939 (1981).
- [28] F. H. L. Essler and I. Affleck, cond-mat/0410487.